Makara Journal of Science

Volume 26
Issue 2 *June*

Article 3

6-30-2022

Co-microencapsulation of Ruellia tuberosa L. and Cosmos caudatus K. Extracts for Pharmaceutical Applications

Choirin Annisa
Chemistry Department, Faculty of Mathematics and Natural Sciences, Universitas Brawijaya, Malang 65145, Indonesia

Sasangka Prasetyawan
Chemistry Department, Faculty of Mathematics and Natural Sciences, Universitas Brawijaya, Malang 65145, Indonesia

Anna Safitri
Research Center for Smart Molecules of Natural Genetic Resources (SMONAGENES), Universitas Brawijaya, Malang 65145, Indonesia, a.safitri@ub.ac.id

Recommended Citation

Annisa, Choirin; Prasetyawan, Sasangka; and Safitri, Anna (2022) "Co-microencapsulation of Ruellia tuberosa L. and Cosmos caudatus K. Extracts for Pharmaceutical Applications," *Makara Journal of Science*: Vol. 26: Iss. 2, Article 3.
DOI: 10.7454/mss.v26i2.1334
Available at: https://scholarhub.ui.ac.id/science/vol26/iss2/3

Makara Journal of Science, 26/2 (2022), 96–106
doi: 10.7454/mss.v26i2.1334

Co-microencapsulation of *Ruellia tuberosa* L. and *Cosmos caudatus* K. Extracts for Pharmaceutical Applications

Choirin Annisa[1], Sasangka Prasetyawan[1], and Anna Safitri[1,2*]

1. Chemistry Department, Faculty of Mathematics and Natural Sciences, Universitas Brawijaya, Malang 65145, Indonesia
2. Research Center for Smart Molecules of Natural Genetic Resources (SMONAGENES), Universitas Brawijaya, Malang 65145, Indonesia

E-mail: a.safitri@ub.ac.id

Received March 17, 2022 | Accepted June 21, 2022

Abstract

This study aims to co-microencapsulate the *Ruellia tuberosa* L. and *Cosmos caudatus* K. extracts, with chitosan–sodium tripolyphosphate (Na-TPP) as coating material. α-Amylase inhibition and antioxidant assays were conducted to determine the potential of microcapsules used as antidiabetic agents. The microcapsules were manufactured under the influences of pH, Na-TPP concentration, and stirring time. The optimum microencapsulation conditions were selected based on the highest encapsulation efficiency. The optimum microencapsulation conditions were a pH of 4, Na-TPP concentration of 0.15% (w/v), and stirring time of 60 min. The microcapsules exhibited an IC_{50} (inhibitory concentration) value of 223.64 ± 0.81 μg/mL and an α-amylase inhibition and antioxidant activity of 104.05 ± 0.88 μg/mL. The test for the release of bioactive compounds from microcapsules was conducted in HCl pH 1.2 and phosphate buffer pH 7.4 for 30–120 min. Results showed that 5.99% and 58.96% of bioactive compounds were released at pH 1.2 and 7.4, respectively, in 120 min. The Fourier transform infrared spectra showed the P=O functional group vibrations from Na-TPP at 1,213.71 cm^{-1} and C–N stretching vibrations from chitosan at 1,155.23 cm^{-1}. Characterization with scanning electron microscopy and particle size analysis indicated that the microcapsules were spherical and had a mean diameter of 132.08 μm. The current study demonstrated that co-microencapsulation is a promising multifaceted approach for the enhancement of the pharmaceutical applications of plant extract combinations.

Keywords: Ruellia tuberosa L., Cosmos caudatus K., co-microencapsulation, chitosan, Na-TPP

Introduction

Ruellia tuberosa L. or *pletekan* is a widely distributed herbal plant in Indonesia. This plant has been used as an antidiuretic, antidiabetic, analgesic, antipyretic, and antihypertensive [1, 2]. In general, *R. tuberosa* L. has been used as a natural antidiabetic remedy [2]. The bioactive compounds in the root extract of *R. tuberosa* L. are phytosterols and flavonoids. Phytosterol compounds have antioxidant activity needed in diseases associated with free radicals, such as diabetes [3]. The flavonoid compounds in the root extract of *R. tuberosa* L., such as sorbifolin, cirsimarin, cirsimaritin, and cirsiol 4′-glucoside, have been proposed to have antidiabetic activity [4]. Moreover, both in vivo and in silico studies have been conducted to explore the potential of the *R. tuberosa* L. extract as an antidiabetic agent [4–6].

Apart from *R. tuberosa* L., *Cosmos caudatus* K. or *kenikir*, an herb from Latin America, has also been widely proposed to have various biological functions. *C. caudatus* K. plants are found in East Africa, Europe, and Southeast Asia (e.g., Indonesia) [7, 8]. This plant has antidiabetic, antihypertensive, and anti-inflammatory activities [9]. Flavonoids, polyphenols, saponins, alkaloids, and tannins are the bioactive compounds found in *C. caudatus* K. [10]. The flavonoid compounds in the leaf extract of *C. caudatus* K., such as genistin, oroxin B, and quercetin (QE), have antidiabetic and antioxidant activities proven through in vitro studies [11].

The number of diabetes mellitus (DM) cases in Indonesia has increased over the past 6 years [12]. More than 90% of cases worldwide are caused by Type 2 DM [6]. Based on the International Diabetes Federation report, the number of people with Type 2 DM was 7.3 million in 2009 and increased to 10.3 million in 2017 [12]. Type 2 DM is a metabolic disorder caused by the resistance of body cells to insulin [6, 13]. As a result, insulin secreted by pancreatic β-cells cannot maintain normal blood glucose levels [6]. The development of Type 2 diabetes is also influenced by postprandial hyperglycemia, which is an

increase in blood glucose levels because of carbohydrate absorption [14]. α-Amylase is one of the targeted enzymes in the treatment of Type 2 DM. α-Amylase hydrolyzes the α-glycosidic bonds in starch into oligosaccharides (i.e., lactose, maltose, and sucrose). α-Amylase inhibition prevents further digestion of carbohydrates; as a result, the body absorbs less glucose [15]. Furthermore, in Type 2 DM, hyperglycemia increases reactive oxygen species production and oxidative stress. Increased oxidative stress induces the development of complications, such as myocardial injury, diabetic retinopathy, and cardiovascular disease. Therefore, antioxidants are also needed for Type 2 DM treatment [16].

Several previous studies proposed that *R. tuberosa* L. and *C. caudatus* K. have antidiabetic and antioxidant activities [3–6, 11]. As a result, the use and development of herbal plants in medicine have increased. However, the two plants have never been combined. Therefore, further research is needed to determine the biological activity of the combination of *R. tuberosa* L. and *C. caudatus* K. as a new drug candidate for Type 2 DM.

In developing antidiabetic drug candidates, oral bioavailability, which is the number of bioactive compounds that can reach the systemic circulation, needs to be considered. Therefore, the molecular properties of the bioactive compounds in the *R. tuberosa* L. and *C. caudatus* K. extracts, which limit their bioavailability, need to be understood [17]. Cirsimarin is a bioactive compound with low permeability, whereas QE is a hydrophobic compound with low solubility. As a result, fewer bioactive compounds are absorbed by the digestive tract. Furthermore, the expected efficacy is not achieved because of the lack of bioactive compounds in the systemic circulation [18]. The bioavailability of bioactive compounds in *R. tuberosa* L. and *C. caudatus* K. could be improved using the encapsulation technique [19]. The microencapsulation technique is used to retain the active ingredients in plant extracts and control the release of extracts entering the systemic circulation [20]. Microencapsulation is defined as the coating of the core material by polymers to produce particles with the size of 5–5,000 μm [21]. For microencapsulation, spray drying is the most frequently used method. The extract is dispersed into a polymer solution and sprayed in a high-temperature chamber. Then, the atomization and evaporation processes of the solvent are conducted to obtain dry particles [22]. A common technique used to prepare coating solutions is the ionic gelation technique [23].

The ionic gelation technique is based on the formation of a polyelectrolyte complex between polycations and polyanions. Chitosan is a biopolymer that is widely used as a coating material in microencapsulation [23]. Chitosan is nontoxic and biodegradable and has low solubility in water [20–24]. Moreover, the amino group of chitosan can be protonated at pK_a below 6.5. Then, these polycations form cross-links with polyanions, such as sodium tripolyphosphate (Na-TPP) [23, 25]. The addition of Na-TPP as a cross-linking agent strengthens the chitosan matrix, resulting in a stable coating material [26]. Several factors, including the solubility of chitosan, Na-TPP concentration, and stirring time, influence microencapsulation. Chitosan is soluble in organic acid solvents at pH 4–6.5 [24]. The pH of the acetic acid solution, Na-TPP concentration, and stirring time affect the microencapsulation efficiency [27–29].

This study aims to investigate the encapsulation process using the spray drying technique. The coating material used is chitosan polymer with Na-TPP as the cross-linking agent. Several factors, such as pH, Na-TPP concentration, and stirring time, were investigated to determine the optimum microencapsulation conditions. Furthermore, to determine its potential as a Type 2 DM drug, activity tests were conducted on the resulting microcapsules under the optimum microencapsulation conditions through α-amylase inhibition and antioxidant assays.

Materials and Methods

Materials and instruments. The materials used in this research were *R. tuberosa* L. root powder and *C. caudatus* K. leaf powder obtained from UPT Laboratorium Herbal Materia Medica, Batu, East Java, Indonesia. The chemicals used in this research include ethyl alcohol (99.7%), glacial acetic acid (secondary pharmaceutical standard), α-amylase from *Aspergillus oryzae* (≥150 units/mg protein), chitosan (low Sabarudin weight, 50,000–190,000 kDa), Na-TPP (technical grade, 85%), aluminum chloride ($AlCl_3$), 3,5-dinitrosalicylic acid (DNS) reagent (≥98%, high-performance liquid chromatography grade), 2,2-diphenyl-1-picrylhydrazyl (DPPH, reagent grade), Tween-80, and soluble starch (from potato, American Chemical Society grade). The instruments used in this research were the Shimadzu UV–Vis spectrophotometer, Shimadzu Prestige 21 FTIR spectrometer, CILAS 1090 particle size analyzer (PSA), and SEM TM 3000 Hitachi.

Extract preparations. A total of 250 g of *R. tuberosa* L. root powder was macerated three times in 1 L of 96% ethanol for 24 h. Then, the extracts were filtered and concentrated using a rotary evaporator at 50 °C and 120 rpm. The extracts were stored at 4 °C for further use.

A total of 250 g of *C. caudatus* K. leaf powder was dissolved in 1 L of 96% ethanol solvent and macerated three times for 24 h. The extract was filtered using Whatman filter paper. Then, the solvent was evaporated using a rotary evaporator at 68 °C and 120 rpm. The concentrated extract obtained was stored at 4 °C for subsequent use.
R. tuberosa L. and *C. caudatus* K. extracts weighing 1 g each were dissolved in 0.2 mL of distilled water and 4.8

mL of ethanol p.a. Then, 100 mL of Tween-80 0.1% (w/v) was added and stirred at 500 rpm. Furthermore, the mixture was concentrated to obtain a combination of *R. tuberosa* L. and *C. caudatus* K. extracts.

Co-microencapsulation of *R. tuberosa* L. and *C. caudatus* K. Extracts. The preparation and co-microencapsulation of *R. tuberosa* L. and *C. caudatus* K. extracts were conducted by weighing 500 mg of the combined extract. Then, the combined extract was dissolved in 0.4 mL of distilled water and 9.6 mL of ethanol p.a. The sample solution was mixed with 0.1% (w/v) chitosan in 1% (w/v) acetic acid solution (pH 3, 4, 5, and 6). Subsequently, 0.1% (w/v) Na-TPP solution was added and stirred at a constant speed of 900 rpm for 60 min. Finally, the solution was spray-dried with an inlet temperature of 105 °C, outlet temperature of 85 °C, and air pressure of 1 bar.

The parameters affecting co-microencapsulation were investigated in several stages. First, the effect of the variation of pH was analyzed. The optimum pH condition was used to determine the effect of Na-TPP concentration at 0.15%, 0.20%, 0.25%, and 0.3% (w/v). Meanwhile, the other conditions remained the same. Finally, the same procedure was used to determine the effect of stirring time (i.e., 30, 60, 90, and 120 min) under optimum pH and Na-TPP concentration conditions. The optimum conditions for each parameter were determined using the encapsulation efficiency (EE, %).

Encapsulation efficiency. EE indicates the effectiveness of the coating material in encapsulating and protecting the extract [30]. EE was calculated using the following equation:

$$Encapsulation\ Efficiency\ (\%) = \frac{Total\ flavonoid\ content\ in\ microcapsules}{Total\ flavonoid\ content\ in\ extracts} \times 100\%$$

The total flavonoid content (TFC) was determined using the $AlCl_3$ colorimetric method. For TFC determination, the standard curves of QE solutions with various concentrations (5–20 µg/mL) were obtained. The QE standard solution and samples (extracts and microcapsules) were pipetted (as much as 0.6 mL) and placed in a test tube. Then, the solution was mixed with 0.6 mL of 2% $AlCl_3$ and incubated at room temperature for 23 min. The mixed solution was measured using a UV–Vis spectrophotometer at the maximum wavelength of QE (420 nm). Experiments were conducted in triplicate. The TFC of each sample was calculated using the standard QE curve ($y = 0.0474x + 0.0076$, $R^2 = 0.9985$) and expressed as mg QE/g sample.

In vitro α-amylase inhibitory activity. All samples were prepared with various concentrations (i.e., 100–500 µg/mL for the combined extract and microcapsules and 10–50 µg/mL for acarbose). Then, 250 µL of the sample solution was mixed with 250 µL of the α-amylase enzyme solution (50 µg/mL) and incubated at 37 °C for 30 min. Afterward, 250 µL of 1% starch solution (w/v) was added and incubated at 25 °C for 10 min. Subsequently, the solution was mixed with 500 µL DNS reagent and was incubated in boiling water for 5 min until the solution turned brownish red. Finally, the solution was cooled, and 5 mL of distilled water was added. The absorbance of the mixed solution was measured at a wavelength of 480 nm using a UV–Vis spectrophotometer. Experiments were conducted in triplicate. The calculation of the percent inhibition of the α-amylase enzyme activity of the sample was conducted using the following equation:

$$Percentage\ of\ Enzyme\ Inhibition\ (\%) = \frac{Absorbance\ control - Absorbance\ sample}{Absorbance\ control} \times 100\%$$

The sample concentration and percent inhibition were plotted on the *x*- and *y*-axes, respectively, in the linear regression equation. The calculated results were expressed as the IC_{50} (inhibitory concentration) value, which is the capability of the inhibitor at a particular concentration to inhibit 50% of α-amylase enzyme activity.

Antioxidant activity assay using the DPPH method. Samples with various concentrations (i.e., 10–50 µg/mL for the *R. tuberosa* L. and *C. caudatus* K. extracts, 40–120 µg/mL for the microcapsules, and 1–13 µg/mL for ascorbic acid) were prepared. A 50 µg/mL DPPH solution was added to each solution. The mixed solution was incubated at room temperature for 30 min and kept in the dark. Then, the absorbance was measured using a UV–Vis spectrophotometer at 516 nm. Experiments were conducted in triplicate. The percentage of antioxidant activity was calculated using the following formula:

$$Percentage\ of\ Enzyme\ Inhibition\ (\%) = \frac{Absorbance\ control - Absorbance\ sample}{Absorbance\ control} \times 100\%$$

The IC_{50} value was calculated using the linear regression equation, with the sample concentration on the *x*-axis and the percent antioxidant activity on the *y*-axis.

In vitro release study. In vitro release assay of the microcapsule samples was conducted in two types of medium, namely, simulated gastric fluid (HCl pH 1.2) and simulated intestinal fluid (phosphate buffer pH 7.4). The 2.5 mg microcapsule sample was immersed in 10 mL of the medium at 37 °C and stirred at a slow speed of 100 rpm. Then, 10 mL samples were taken at 30, 60, 90, and

120 min. Experiments were conducted in triplicate. The concentration of the extract released from the microcapsules was calculated as the TFC and expressed as the percentage release using the following equation:

$$Percentage\ of\ Enzyme\ Inhibition\ (\%) = \frac{Absorbance\ control - Absorbance\ sample}{Absorbance\ control} \times 100\%$$

FTIR, particle size distribution, and SEM analysis. FTIR analysis of the dry samples in the form of KBr pellets was conducted using a Fourier transform infrared (FTIR) spectrophotometer at 4,000–400 cm^{-1}. The particle size distribution of the microcapsules was determined using a PSA. The shape and morphology of the microcapsules were observed using scanning electron microscopy (SEM), with magnifications of ×7,000 to ×15,000.

Data analysis. The results were expressed as the mean ± standard error of the mean. Statistical analysis was performed using the Statistical Package for the Social Sciences v.26 software, followed by one-way analysis of variance and Tukey's honestly significant difference, to determine the significant difference. $p < 0.05$ was considered a significant difference.

Results and Discussion

R. tuberosa L. and *C. caudatus* K. microcapsules were produced using the spray drying method under the influences of pH, stirring time, and Na-TPP concentration. The resulting data are shown in Figure 1. The optimum microencapsulation conditions were achieved at pH 4, 0.15% Na-TPP concentration (b/v), and 60 min stirring time, with 96.25% EE.

The microcapsules prepared at pH 4 exhibited the highest EE. Chitosan is soluble in acidic pH with pK_a below 6.3. At pH 4, chitosan received more proton donors. Thus, NH_3^+ ions increased because of the protonation of the amine group (NH_2) of chitosan. As a result, more ionic bonds can be formed with the phosphate ion ($P_3O_{10}^{5-}$) of Na-TPP [31]. Therefore, the microcapsule matrix formed is strong, and the number of encapsulated bioactive compounds increases, thereby increasing the EE.

The results of this study are similar to those of previous studies. At pH 4, a stoichiometric equilibrium of the charge density of biopolymers with opposite signs is achieved. Thus, in the design of microcapsules containing chitosan, pH 4 is the most effective pH value [28]. Meanwhile, at pH < 4, increasing protonation of NH_2 causes strong intramolecular repulsion, which will reduce the bond strength between chitosan and Na-TPP [32]. According to a previous study [33], at pH > 4, the microcapsule matrix formed is weak because of the deprotonation of NH_2.

In this study, the optimum microencapsulation conditions were obtained at the Na-TPP concentration of 0.15% (w/v). Figure 1B shows that the higher the Na-TPP concentration used, the lower the EE of the microcapsules. Meanwhile, the chitosan concentration used in this study was 0.1% (w/v) under the same conditions. The same results were obtained in previous studies [34, 35], i.e., at a high Na-TPP concentration, the number of $P_3O_{10}^{5-}$ ions that would form ionic bonds with NH_3^+ was not balanced. As a result, the microcapsule matrix formed is weak. Therefore, the capability to absorb *R. tuberosa* L. and *C. caudatus* K. extracts is weak.

Stirring time is also a factor observed in this study. The highest EE was obtained at a stirring time of 60 min. Increasing the stirring time can reduce the size of the resulting microcapsules. A high-intensity collision will produce small particles, resulting in a large particle surface area [30]. Therefore, the adsorbed extracts of *R. tuberosa* L. and *C. caudatus* K. increased. However, prolonged stirring can cause microcapsule aggregation. This result is consistent with those of previous studies [36–38].

For the first biological assay, the antidiabetic activity of the samples was determined by an α-amylase inhibition test. The samples used in this test were the combination of *R. tuberosa* L. and *C. caudatus* K. extracts under the optimum microencapsulation conditions and acarbose. The results of the study are shown in Table 1.

The IC_{50} value of *R. tuberosa* L. and *C. caudatus* K. extracts was 121.48 ± 0.88 µg/mL in terms of α-amylase inhibitory activity, whereas that of microcapsules was 223.64 ± 0.81 µg/mL. The inhibitory activity of the extract against α-amylase was higher than that of the microcapsules because of the retention of some bioactive compounds in the microcapsules. As a result, the microcapsules did not release bioactive compounds entirely. The primary purpose of microencapsulation is not to increase biological activity but to maximize protection against bioactive compounds [28]. Moreover, with microencapsulation, the release of bioactive compounds can be conducted in a controlled manner [39]. Thus, the microcapsules of *R. tuberosa* L. and *C. caudatus* K. acted as α-amylase inhibitors.

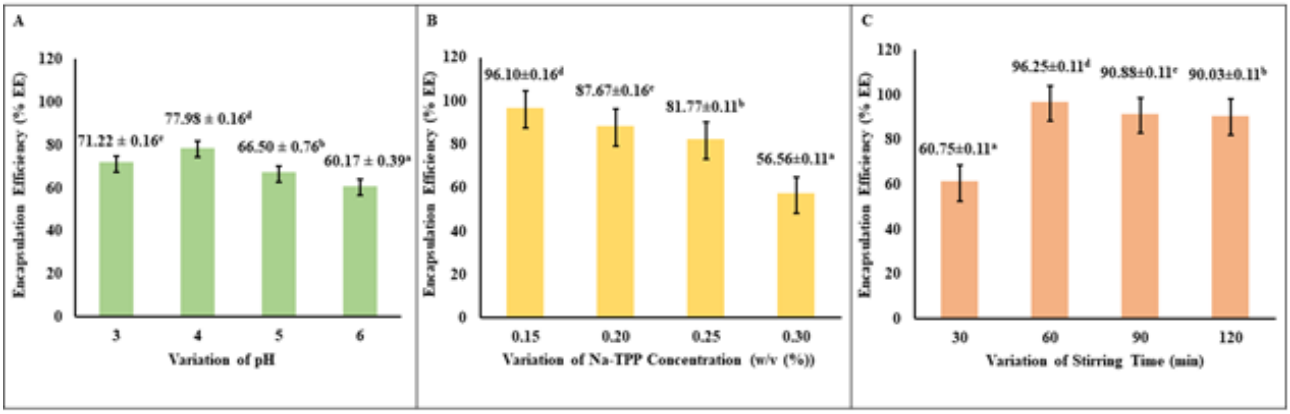

Figure 1. Encapsulation Efficiency of *Ruellia tuberosa* L. and *Cosmos caudatus* K. Microcapsules Prepared at Different (A) pH values, (B) Na-TPP Concentrations (w/v (%)), and (C) Stirring Times

Table 1. IC_{50} Values of *Ruellia tuberosa* L. and *Cosmos caudatus* K. Extracts, Microcapsules, and Acarbose on the α-amylase Inhibition Assay

Samples	IC_{50} value (µg/mL)
R. tuberosa L. and *C. caudatus* K. extracts	121.48 ± 0.88
Microcapsules at pH 4, 0.15% (b/v) Na-TPP concentration, and 60 min stirring time	223.64 ± 0.81
Acarbose	19.58 ± 0.12

Table 2. Antioxidant Activity of *R. tuberosa* L. and *C. caudatus* K. Extracts, Microcapsules, and Ascorbic Acid

Samples	IC_{50} value (µg/mL)
R. tuberosa L. and *C. caudatus* K. extracts	33.47 ± 0.03
Microcapsules at pH 4, 0.15% (b/v) Na-TPP concentration, and 60 min stirring time	104.05 ± 0.88
Ascorbic acid	3.05 ± 0.05

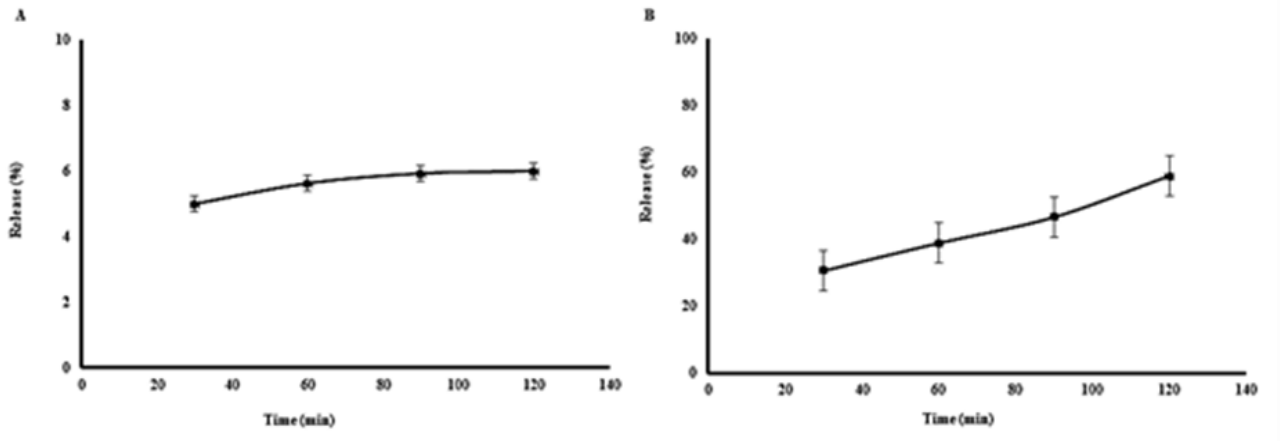

Figure 2. Release Profile of the *R. tuberosa* L. and *C. caudatus* K. Microcapsules Prepared under the Optimum Conditions of pH 4, 0.15% (b/v) Na-TPP Concentration, and 60 min Stirring Time at (A) pH 1.2 and (B) 7.4

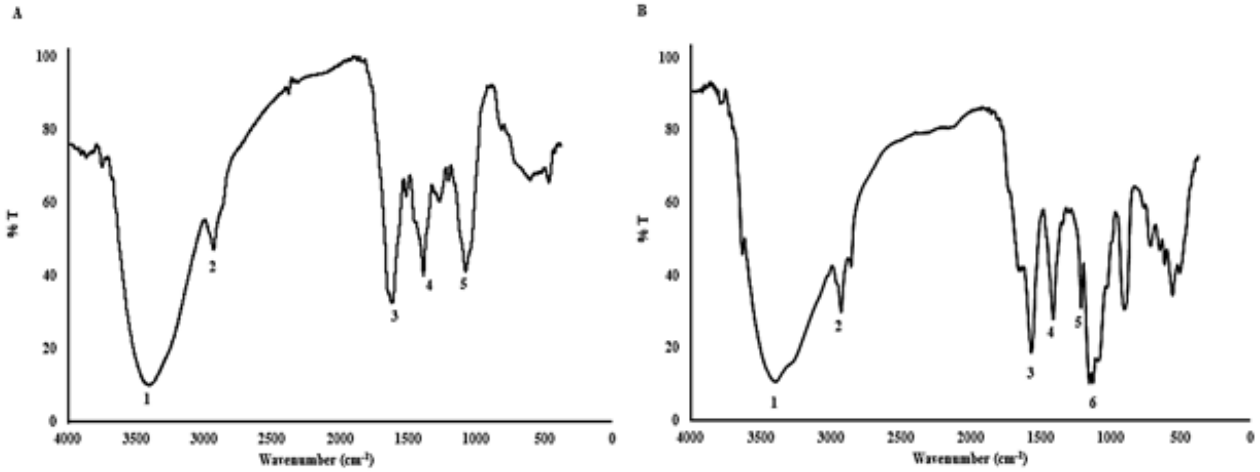

Figure 3. FTIR Spectra of (A) *R. tuberosa* L. and *C. caudatus* K. Extracts and (B) *R. tuberosa* L. and *C. caudatus* K. Microcapsules Prepared under the Optimum Conditions of pH 4, 0.15% (b/v) Na-TPP Concentration, and 60 min Stirring Time

Table 3. Assignment of FTIR Spectra

Peak Number	Assignment for *R. tuberosa* L. and *C. caudatus* K. extracts [53–56]	Assignment for *R. tuberosa* L and *C. caudatus* K. microcapsules [28, 53–56]
1	3,400.09 cm^{-1} for O–H alcohol	3,395.81 cm^{-1} for alcohol
2	2,928.01 cm^{-1} for C–H methylene	2,925.16 cm^{-1} for C–H methylene
3	1,617.32 cm^{-1} for C=C aromatic and C=O ketone	1,570.26 cm^{-1} for C=C aromatic
5	1,386.28 cm^{-1} for C–H alkene	1,411.95 cm^{-1} for C=C aromatic
6	1,076.79 cm^{-1} for C–O–C aryl alkyl ether	1,213.71 cm^{-1} for P=O
		1,155.23 cm^{-1} for C–N

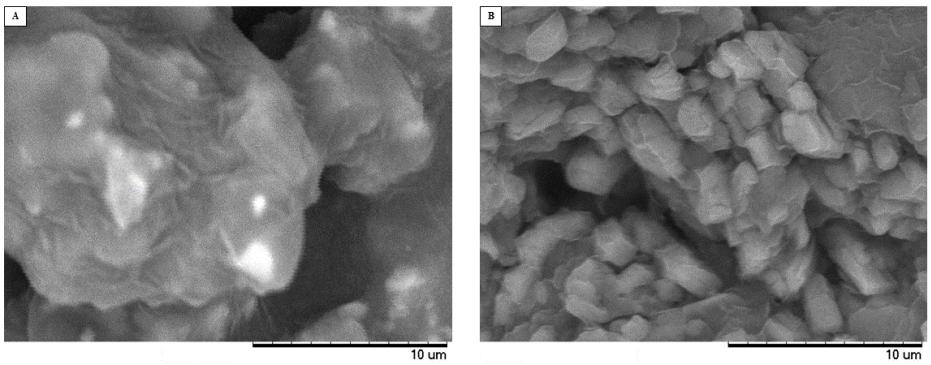

Figure 4. SEM Images of (A) *R. tuberosa* L. and *C. caudatus* K. Extracts and (B) *R. tuberosa* L. and *C. caudatus* K. Microcapsules Prepared under the Optimum Conditions of pH 4, 0.15% (b/v) Na-TPP Concentration, and 60 Min Stirring Time. The Magnification was ×7,000

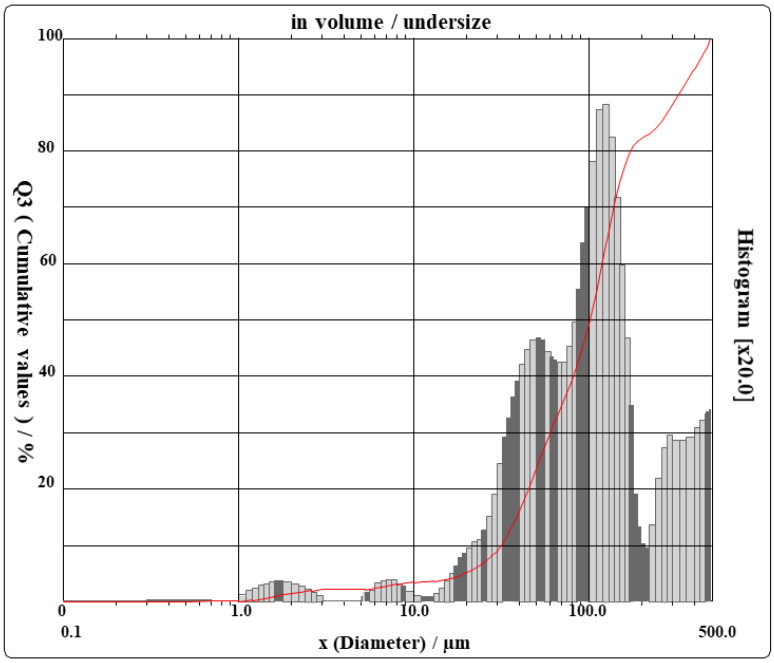

Figure 5. Particle Size Distribution of *R. tuberosa* L. and *C. caudatus* K. Microcapsules Prepared under the Optimum Conditions of pH 4, 0.15% (b/v) Na-TPP Concentration, and 60 Min Stirring Time

Acarbose, as a reference, had an IC_{50} value of 19.58 ± 0.12 µg/mL. The smallest IC_{50} value indicates the highest α-amylase inhibitory activity. Compared with extracts and microcapsules, acarbose exhibited the best inhibitory activity against α-amylase. These results are consistent with those of previous studies because acarbose is a competitive inhibitor for α-amylase [40]. Furthermore, although the *R. tuberos*a L. and *C. caudatus* K. extracts contain several bioactive compounds [3, 10], not all of these compounds have inhibitory activity against α-amylase [28]. Flavonoid compounds are bioactive compounds that can act as α-amylase inhibitors. Flavonoids bind to α-amylase covalently and alter their activity because of their capability to form quinones or lactones that react with the nucleophilic group of the enzyme [41].

For the second biological assay, a test was conducted to confirm the antioxidant activity of the samples. The antioxidant activity test results are shown in Table 2. The samples used were the combination of *R. tuberosa* L and *C. caudatus* K. extracts under the optimum microencapsulation conditions and ascorbic acid as a positive reference.

The antioxidant activity test was conducted using the DPPH reagent. The DPPH radical is an organic compound containing unstable nitrogen and produces a dark purple solution color [42]. Antioxidants, such as ascorbic acid, act as reducing agents to stabilize these free radicals. As a result, a colorless solution is obtained [43, 44]. As previously reported, antioxidant activity is also required to treat diseases associated with free radical involvement, such as diabetes [45]. Based on the IC_{50} data shown in Table 3, the antioxidant activity of microcapsules (104.05 ± 0.88 µg/mL) was lower than those of extracts (33.47 ± 0.03 µg/mL) and ascorbic acid (3.05 ± 0.05 µg/mL). Nevertheless, the *R. tuberosa* L. and *C. caudatus* K. microcapsules are categorized as active antioxidants (100 < IC_{50} value < 150 µg/mL). Moreover, the *R. tuberosa* L. and *C. caudatus* K. extracts are classified as very active antioxidants (IC_{50} < 50 mg/mL) but are less active than ascorbic acid [42].

The in vitro release study is a crucial parameter used to test the capability of microcapsules for drug administration in the systemic circulation [46]. In the determination of oral drug candidates, the test for the release of bioactive compounds from the microcapsule matrix was conducted at pH 1.2 (artificial gastric fluids) and pH 7.4 (artificial intestinal fluids). In this study, the release of extracts was triggered by pH stimulation. In general, under acidic pH conditions in gastric fluids, microcapsule formulations can maintain the release of the bioactive compounds for 15 min to 2 h. Furthermore, the active ingredients are released when they reach the intestines under alkaline pH conditions. The release of bioactive compounds in the intestinal organs lasts for 2 h until they penetrate the bloodstream [47, 48]. Therefore, the release test was conducted in acid and alkaline media for 2 h.

The release profile study at pH 1.2 (Figure 2) showed that the percentage release of the *R. tuberosa* L. and *C. caudatus* K. extracts was 4.99% in the first 30 min and increased to 5.99% at 120 min. At pH 1.2, the NH_2 group

is protonated into NH_3^+; thus, chitosan becomes positively charged. Under acidic pH conditions, H^+ ions interact with cations on the surface of chitosan. As a result, the chitosan–Na-TPP cleavage process was limited, which slowed the release of the extract [49]. By contrast, the percentage release of extract by microcapsules at pH 7.4 was 30.60% in 30 min and reached 58.96% in 120 min. More extracts were released under alkaline pH conditions because of the deprotonation of NH_3^+ ions from chitosan into a non-ionized state, resulting in the breakdown of the bond between chitosan and Na-TPP matrix [49, 50].

Microcapsules protect and control the release of extracts when they reach the systemic circulation [20, 51]. Microcapsules are administered through absorption in the gastrointestinal tract (Sabra & Billa, 2020). Chitosan–Na-TPP-based microcapsules are expected to be more stable in acidic pH conditions in gastric fluids than in alkaline pH conditions. Moreover, the amount of extracts released from the coating matrix is expected to be higher at alkaline pH conditions in intestinal fluids so that a larger amount of extracts can be absorbed into the bloodstream and the required therapeutic effect can be achieved [46, 49]. Although the results of this study are consistent with those of previous studies [46, 49], the percentage of *R. tuberosa* L. and *C. caudatus* K. extracts released at pH 7.4 was only 58.98%. Under alkaline pH conditions, the retention of the extract in the microcapsules was caused by the electrostatic repulsion of the ionized group of chitosan [52]. Therefore, the microcapsules could not release all of the extracts at 120 min.

The FTIR spectra enable the identification of functional groups in the *R. tuberosa* L. and *C. caudatus* K. microcapsules. Figure 3 shows the FTIR spectra. Meanwhile, Table 3 lists the assignments of the absorption functional groups.

The spectral analysis showed that the *R. tuberosa* L. and *C. caudatus* K. extracts exhibited stretching vibration of the O–H group at 3,400.09 cm^{-1}. Then, absorption at 2,928.01 cm^{-1} indicated the C–H stretching vibration of the methylene group. The C=C stretching aromatic and C=O stretching ketone vibrations were detected at 1,617.32 cm^{-1}. Furthermore, absorption peaks detected at 1,386.28 and 1,076.79 cm^{-1} were interpreted as C–H stretching vibrations of alkenes and C–O–C stretching vibrations of aryl alkyl ethers, respectively [53–56]. According to previous studies [28, 30, 57], stretching vibrations at approximately 1,386.28 and 1,076.79 cm^{-1} indicated the typical absorption of the *R. tuberosa* L extract. Meanwhile, the wavenumber at approximately 1,617.32 cm^{-1} indicated the specific absorption of the *C. caudatus* K. extract.

By contrast, the microcapsule FTIR spectra indicated a shift in the stretching vibrational spectra of the O–H alcohol, C–H methylene, and C=C aromatic groups. Moreover, the occurrence of new absorption indicated the presence of P=O functional group vibrations from Na-TPP (1,213.71 cm^{-1}) and C–N stretching vibrations from chitosan (1,155.23 cm^{-1}) [28]. The occurrence of these two types of absorption refers to the polymer and cross-linker used to manufacture the microcapsules.

Characterization was then conducted to determine the surface morphology and size of the obtained microcapsules. Figure 4A and 4B shows the differences in SEM results between extracts and microcapsules. The microcapsules were spherical and nearly uniform in size and had rough surfaces. In this study, the morphology of the obtained microcapsules was similar to that in a previous study [28]. Microcapsule analysis using a PSA aims to determine the particle size distribution. The mean diameter of the microcapsules was 132.08 µm, as shown in Figure 5. The particle size distribution was determined to be polymodal. The polymodal distribution is particularly prevalent for granular particles [58]. Nevertheless, the microcapsules obtained in this study did not meet the requirements for the particle size produced from the spray drying process (10–100 µm) [59]. The inlet temperature of 105 °C used in spray drying was high. At high temperatures, water vapor is difficult to diffuse through the particle surface because of the formation of a crust layer on the droplet surface. As a result, the microcapsule particle size is large [60].

Conclusion

In this study, microencapsulation of the *R. tuberosa* L. and *C. caudatus* K. extracts was successfully conducted. The investigated parameters include pH variation, Na-TPP concentration, and stirring time. The microcapsules were produced using the spray drying technique under the optimum microencapsulation conditions of pH 4, 0.15% (w/v) Na-TPP concentration, and 60 min stirring time. The microcapsules have inhibitory activity against α-amylase with an IC_{50} value of 223.64 ± 0.81 µg/mL. Furthermore, the microcapsules have antioxidant activity with an IC_{50} value of 104.05 ± 0.88 µg/mL. The in vitro release test showed that the *R. tuberosa* L. and *C. caudatus* K. extracts were more easily released at pH 7.4 than at pH 1.2. FTIR analysis showed the cross-linking between chitosan and Na-TPP. SEM analysis showed that the microcapsules were spherical and nearly uniform in size and had rough surfaces. Meanwhile, particle size analysis showed that the microcapsules had a particle diameter of 132.08 µm.

Acknowledgments

This work was supported by *Penelitian Tesis Magister* grant, year of 2022, and was part of *Hibah Penelitian Unggulan*, Universitas Brawijaya, Indonesia, year of 2021.

References

[1] Samy, M.N., Sugimoto, S., Matsunami. K., Otsuka, H., Kamel, M.S. 2015. Chemical constituents and biological activities of genus Ruellia. Int. J. Pharmacogn. 2(6): 270–279, https://doi.org/10.13040/IJPSR.0975-8232.IJP.2(6).270-79.

[2] Roosdiana, A., Permata, F.S., Fitriani, R.I., Umam, K., Safitri, A. 2020. *Ruellia Tuberosa* L. Extract Improves Histopathology and Lowers Malondialdehyde Levels and TNF Alpha Expression in the Kidney of Streptozotocin-Induced Diabetic Rats. Vet. Med. Int. 2020: 1–7, https://doi.org/10.1155/2020/8812758.

[3] Safitri, A., Roosdiana, A., Rosyada, I., Evindasari, C.A., Muzayyana, Z., Rachmawanti, R. Phytochemicals Screening and Anti-Oxidant Activity of Hydroethanolic Extracts of *Ruellia Tuberosa* L. IOP Conf. Ser. Mater. Sci. Eng. 509: 1–8, https://doi.org/10.1088/1757-899X/509/1/ 01201 7.

[4] Safitri, A., Roosdiana, A., Arrochmah, N., Nur'Adya, S.S. 2019. Anti-diabetic properties of root extracts of *Ruellia tuberosa* L: effects on serum enzyme activity. J. Phys. Conf. Ser. 1374(1): 012030, https://doi.org/10.1088/1742-6596/1374/1/012030.

[5] Safitri, A., Sari, D.R.T., Fatchiyah, F., Roosdiana, A. 2021. Modeling of Aqueous Root Extract Compounds of *Ruellia tuberosa* L. for Alpha-Glucosidase Inhibition Through in Silico Study. Makara J. Sci. 25(1): 51–60, https://doi.org/10.7454/mss.v25i1.1223.

[6] Safitri, A., Srihardyastutie, A., Roosdiana, A., Aulanni'am, A., Octaviana, E.N.L. 2019. Effects of Root Extract of *Ruellia tuberosa* L. on Kidneys of Diabetic Rats. J. Math. Fundam. Sci. 51(2): 127–137, https://doi.org/10.5614/j.math.fund.sci.2019.51.2.3.

[7] Moshawih, S., Cheema, M.S., Ahmad, Z., Zakaria, Z.A., Hakim, M.N. 2017. A Comprehensive Review on *Cosmos caudatus* (Ulam Raja): Pharmacology, Ethnopharmacology, And Phytochemistry. Irjes. 1(1): 14–31.

[8] Ramadhan, F., Mukarramah, L., Oktavia, F.A.R.H., Yulian, R., Annisyah, N.H., Asyiah, I.N. 2018. Flavonoids from Endophytic Bacteria of *Cosmos caudatus* Kunth. Leaf as Anticancer and Antimicrobial. Asian J. Pharm. Clin. Res. 11(1): 200–204, https://doi.org/10.22159/Ajpcr.2018.V11i1.21987.

[9] Cheng, S.-H., Ismail, A., Anthony, J., Ng, O.C., Hamid, A.A., Yusof, B.-N.M. 2016. Effect of *Cosmos caudatus* (Ulam Raja) Supplementation in Patients with Type 2 Diabetes: Study Protocol for a Randomized Controlled Trial. BMC Complement. Altern. Med. 16(1): 1–8, https://doi.org/10.1186/S12906-016-1047-7.

[10] Bunawan, H., Baharum, S.N., Bunawan, S.N., Amin, N.M., Noor, N.M. 2014. *Cosmos caudatus* Kunth: A Traditional Medicinal Herb. Global J. Pharmacol. 8(3): 420–426, https://doi.org/10.5829/idosi.gjp.2014.8.3.8424.

[11] Firdaus, M.D., Artanti, N., Hanafi, M., Rosmalena. 2021. Phytochemical Constituents, and In Vitro Antidiabetic and Antioxidant Properties of Various Extracts of *Kenikir* (*Cosmos caudatus*) Leaves. Pharmacogn. J. 13(4): 890–895, https://doi.org/10.5530/Pj.2021.13.114.

[12] Arifin, B., Asselt, A.D.I.V., Setiawan, D., Atthobari, J., Postma, M.J., Cao, Q. 2019. Diabetes Distress in Indonesian Patients with Type 2 Diabetes: A Comparison Between Primary and Tertiary Care. BMC Health Serv. Res. 19(1): 1–11, https://doi.org/10.1186/S12913-019-4515-1.

[13] Aouacheri, O., Saka, S., Krim, M., Messaadia, A., Maidi, I. 2015. The Investigation of the Oxidative Stress-Related Parameters in Type 2 Diabetes Mellitus. Can. J. Diabetes. 39(1): 44–49, https://doi.org/10.1016/j.jcjd.2014.03.002.

[14] Gregg, E.W., Sattar, N., Ali, M.K. 2016. The changing face of diabetes complications. Lancet Diabetes Endocrinol. 4(6): 537–547, https://doi.org/10.1016/S2213-8587(16)30010-9.

[15] Mahmood, N. 2016. A Review of A-Amylase Inhibitors on Weight Loss and Glycemic Control in Pathological State Such as Obesity and Diabetes. Comp. Clin. Pathol. 25(6): 1253–1264, https://doi.org/10.1007/S00580-014-1967-X.

[16] Rahimi-Madiseh, M., Malekpour-Tehrani, A., Bahmani, M., Rafieian-Kopaei, M. 2016. The Research and Development on the Antioxidants in Prevention of Diabetic Complications. Asian Pac. J. Trop. Med. 9(9): 825–831, https://doi.org/10.1016/J.Apjtm.2016.07.001.

[17] Veber, D.F., Johnson, S.R., Cheng, H.-Y., Smith, B. R., Ward, K.W., Kopple, K.D. 2002. Molecular Properties that Influence the Oral Bioavailability of Drug Candidates. J. Med. Chem. 45(12): 2615–2623, https://doi.org/10.1021/jm020017.

[18] Truzzi, F., Tibaldi, C., Zhang, Y., Dinelli, G., D'Amen, E. 2021. An Overview on Dietary Polyphenols and Their Biopharmaceutical Classification System (BCS). Int. J. Mol. Sci. 22(11): 1–23, https://doi.org/10.3390/ijms22115514.

[19] Chen, L., Gnanaraj, C., Arulselvan, P., El-Seedi, H., Teng, H. 2019. A Review on Advanced Microencapsulation Technology to Enhance Bioavailability of Phenolic Compounds: Based on its Activity in the Treatment of Type 2 Diabetes. Trends Food Sci. Technol. 85: 149–162, https://doi.org/10.1016/J.Tifs.2018.11.026.

[20] Mutmainah, Martono, Y., Puspitaningrum, I., Kusmita, L. 2021. Leaf Extract Microencapsulation of Stevia Rebaudiana Bert using Inulin-Chitosan as

Anti Diabetes Diet. J. Trop. Pharm. Chem. 5(3): 203–208, https://doi.org/10.25026/jtpc.v5i3.270.

[21] Ang, L.F., Darwis, Y., Por, L.Y., Yam, M.F. 2019. Microencapsulation Curcuminoids for Effective Delivery in Pharmaceutical Application. Pharm. 11(451): 1–23, https://doi.org/10.3390/pharmaceuticals11090451.

[22] Rojas-Lema, S., Terol, J., Fages, E., Balart, R., Quiles-Carrillo, L., Prieto, C., Torres-Giner, S. 2020. Microencapsulation of Copper (II) Sulfate in Ionically Cross-Linked Chitosan by Spray Drying for the Development of Irreversible Moisture Indicators in Paper Packaging. Polym. 12(9): 1–16, https://doi.org/10.3390/Polym12092039.

[23] Hussain, S.A., Abdelkader, H., Abdullah, N., Kmaruddin, S. 2018. Review on Micro-Encapsulation with Chitosan for Pharmaceuticals Applications. MOJ Curr. Res. Rev. 1(2): 77–84, https://doi.org/10.15406/Mojcrr.2018.01.00013.

[24] Valle, J.A.B., Valle, R. de C.S.C., Bierhalz, A.C.K., Bezerra, F.M., Hernandez, A.L., Lis Arias, M.J. 2021. Chitosan microcapsules: Methods of the production and use in the textile finishing. J. Appl. Polym. Sci. 138(21): 50482, https://doi.org/10.1002/app.50482.

[25] Yousefi, M., Khorshidian, N., Mortazavian, A.M., Khosravi-Darani, K. 2019. Preparation Optimization and Characterization of Chitosan-Tripolyphosphate Microcapsules for the Encapsulation of Herbal Galactagogue Extract. Int. J. Biol. Macromol. 140: 920–928, https://doi.org/10.1016/J.Ijbiomac.2019.08.122.

[26] Putri, A.S., Octavianty, T.D., Wahyudi, N.T., Safitri, A. 2019. Preparation of Nanoparticles from *Curcuma Longa* L. and *Cosmos caudatus* Extracts. J. Phys. Conf. Ser. 1–6, https://doi.org/10.1088/1742-6596/1374/1/012027

[27] Patil, P., Bhoskar, M. 2014. Optimization and Evaluation of Spray Dried Chitosan Nanoparticles Containing Doxorubicin. Int. J. Curr. Pharm. Res. 6(1): 7–15.

[28] Safitri, A., Roosdiana, A., Hitdatania, E., Damayanti, S.A. 2021. In Vitro Alpha-Amylase Inhibitory Activity of Microencapsulated *Cosmos caudatus* Kunth Extracts. Indo. J. Chem. 22(1): 212–222, https://doi.org/10.22146/Ijc.68844.

[29] Ulyarti, U., Lavlinesia, L., Surhaini, S., Nurainun, S., Anggel, T., Lisani, L, Nazarudin, N. 2021. Development of Yam-Starch-Based Bioplastics with the Addition of Chitosan and Clove Oil. Makara J. Sci. 25(2): 91–97, https://doi.org/ 10.7454/mss.v25i2.1155.

[30] Taurina, W., Sari, R., Hafinur, U.C., Wahdaningsih, S., Isnindar, I. 2017. Optimization of Stirring Speed and Stirring Time Toward Nanoparticle Size of Chitosan-Siam Citrus Peel (*Citrus nobilis* L. *Var Microcarpa*) 70% Ethanol Extract. Majalah Obat Tradisional. 22(1): 16–20, https://doi.org/10.22146/Tradmedj.24302.

[31] Bhumkar, D.R. and Pokharkar, V.B. 2006. Studies on Effect of pH on Cross-Linking of Chitosan with Sodium Tripolyphosphate: A Technical Note. AAPS Pharmscitech. 7(2): E138–E143, https://doi.org/10.1208/Pt070250.

[32] Taherian, A., Esfandiari, N., Rouhani, S. 2021. Breast Cancer Drug Delivery by Novel Drug-loaded Chitosan-Coated Magnetic Nanoparticles. Cancer Nanotechnol. 12(1): 15, https://doi.org/ 10.1186/s12645-021-00086-8.

[33] Mattu, C., Li, R., Ciardelli, G. 2013. Chitosan Nanoparticles as Therapeutic Protein Nanocarriers: The Effect of pH on Particle Formation and Encapsulation Efficiency. Polym. Compos. 34(9): 1538–1545, https://doi.org/10.1002/Pc.22415.

[34] [34] Hassani, S., Laouini, A., Fessi, H., Charcosset, C. 2015. Preparation of Chitosan–TPP Nanoparticles Using Microengineered Membranes–Effect of Parameters and Encapsulation of Tacrine. Colloids Surf. Physicochem. Eng. Asp.482: 34–43, https://doi.org/10.1016/J.Colsurfa.2015.04.006.

[35] Aranaz, I., Paños, I., Peniche, C., Heras, Á., Acosta, N. 2017. Chitosan Spray-Dried Microparticles for Controlled Delivery of Venlafaxine Hydrochloride. Mol. 22(11): 1980, https://doi.org/10.3390/molecules22111980.

[36] Ningsih, Z., Lestari, M.L.A.D., Maharin, S.A.R. 2021. Preparation and Characterization of Curcumin Nanoemulsion in Olive Oil-Tween 80 System using Wet Ball Milling Method. ICS Phys. Chem. 1(1): 16–19, https://doi.org/10.34311/Icspc.2021.1.1.16.

[37] Panigrahi, D., Sahu, P.K., Swain, S., Verma, R.K. 2021. Quality by Design Prospects of Pharmaceuticals Application of Double Emulsion Method for PLGA Loaded Nanoparticles. SN Appl. Sci. 3(638), https://doi.org/10.1007/S42452-021-04609-1.

[38] Kusmayadi, A., Adrian, L., Abun, A., Muchtaridi, M., Tanuwiria, U.H. 2019. The Microencapsulation of Mangosteen Peel Extract with Maltodextrin from Arenga Starch: Formulation and Characterization. J. Appl. Pharm. Sci. 9(3): 33–40, https://doi.org/ 10.7324/JAPS.2019.90306.

[39] Suratman, A., Purwaningsih, D.R., Kunarti, E.S., Kuncaka, A. 2020. Controlled Release Fertilizer Encapsulated by Glutaraldehyde-Crosslinked Chitosan Using Freeze-Drying Method. Indo. J. Chem. 20(6): 1414–1421, https://doi.org/10.22146/Ijc.55133.

[40] Rahimzadeh, M., Jahanshahi, S., Moein, S., Moein, M.R. 2014. Evaluation of Alpha-Amylase Inhibition by Urtica Dioica And Juglans Regia Extracts. Iran J. Basic Med. Sci. 17(6): 466–470.

[41] Oyedemi, S.O., Oyedemi, B.O., Ijeh, I.I., Ohanyerem, P.E., Coopoosamy, R.M., Aiyegoro, O.A. 2017. Alpha-Amylase Inhibition and Antioxidative Capacity of Some Antidiabetic Plants used by the Traditional

Healers in Southeastern Nigeria. Sci. World J. 2017: 1–11, https://doi.org/10.1155/2017/3592491.

[42] Souhoka, F.A., Hattu, N., Huliselan, M. 2019. Uji Aktivitas Antioksidan Ekstrak Metanol Biji Kesumba Keling (*Bixa Orellana* L). Indo. J. Chem. Res. 7(1): 25–31, https://doi.org/10.30598//Ijcr.2019.7-Fas.

[43] Garcia, E.J., Oldoni, T.L.C., De Alencar, S.M., Reis, A., Loguercio, A.D., Grande, R.H.M. 2012. Antioxidant Activity by DPPH Assay of Potential Solutions to Be Applied on Bleached Teeth. Braz. Dent. J. 23(1): 22–27, https://doi.org/10.1590/S0103-64402012000100004.

[44] Njus, D., Kelley, P.M., Tu, Y.-J., Schlegel, H.B. 2020. Ascorbic Acid: The Chemistry Underlying its Antioxidant Properties. Free Radic. Biol. Med. 159: 37–43, https://doi.org/10.1016/J.Freeradbiomed.202 0.07.013.

[45] Safitri, A, Fatchiyah, F., Sari, D.R.T., Roosdiana, A. 2020. Phytochemical Screening, In Vitro Anti-Oxidant Activity, and in Silico Anti-Diabetic Activity of Aqueous Extracts of *Ruellia Tuberosa* L. J. Appl. Pharm. Sci. 10 (3): 101–108, https://doi.org/10.7324/JAPS.2020.103013.

[46] Szczęsna, W., Tsirigotis-Maniecka, M., Szyk-Warszyńska, L., Balicki, S., Warszyński, P., Wilk, K.A. 2021. Insight into Multilayered Alginate/ Chitosan Microparticles for Oral Administration of Large Cranberry Fruit Extract. Eur. Polym. J. 160: 1–11, https://doi.org/10.1016/J.Eurpolymj.2021.110776.

[47] Baek, J.-S., Yeo, E.W., Lee, Y.H., Tan, N.S., Loo S.C. 2017. Controlled-release Nanoencapsulating Microcapsules to Combat Inflammatory Diseases. Drug Des. Devel. Ther. 11: 1707–1717, https://doi.org/10.2147/DDDT.S133344.

[48] Cahyono, B., Suzery, M., Hadiyanto, H., Pratiwi, S. B. 2018. Encapsulation Rutin with Chitosan-NATPP using Coaservation Method. Reaktor. 17(4): 215–220, https://doi.org/10.14710/reaktor. 17.4.215-220.

[49] Herdiana, Y., Wathoni, N., Shamsuddin, S., Muchtaridi, M. 2022. Drug Release Study of The Chitosan-Based Nanoparticles. Heliyon. 8(1): 1–16, https://doi.org/10.1016/J.Heliyon.2021.E08674.

[50] Konecsni, K., Low, N.H., Nickerson, M.T. 2012. Chitosan–Tripolyphosphate Submicron Particles as The Carrier of Entrapped Rutin. Food Chem. 134(4): 1775–1779, https://doi.org/10.1016/ J.Foodchem.2012.03.070.

[51] Sabra, R., Billa, N. 2020. Gastrointestinal Delivery of APIs from Chitosan Nanoparticles. In Chitin and Chitosan–Physicochemical Properties and Industrial Applications. IntechOpen. 2–24, https://doi.org/10.5772/intechopen.95363.

[52] Mulia, K., Andrie, Krisanti, E.A. 2018. Effect of Sodium Tripolyphosphate Concentration and Simulated Gastrointestinal Fluids on Release Profile of Paracetamol from Chitosan Microsphere. IOP Conf. Ser. Mater. Sci. Eng. 316: 1–6, https://doi.org/10.1088/1757-899X/316/1/012028.

[53] Abbas, O., Compère, G., Larondelle, Y., Pompeu, D., Rogez, H., Baeten, V. 2017. Phenolic Compound Explorer: A Mid-Infrared Spectroscopy Database. Vib. Spectrosc. 92: 111–118, https://doi.org/10.1016/J.Vibspec.2017.05.008.

[54] Nandiyanto, A.B.D., Oktiani, R., Ragadhita, R. 2019. How to Read and Interpret FTIR Spectroscope of Organic Material. Indo. J. Sci. Technol. 4(1): 97–118, https://doi.org/10.17509/ Ijost.V4i1.15806.

[55] Kartini, K., Lis, A.D.P., Mochammad Arbi, H. 2020. FTIR-based fingerprinting and discriminant analysis of Apium graveolens from different locations. J. Appl. Pharm. Sci. 10(12): 62–67, https://doi.org/10.7324/JAPS.2020.101208.

[56] Manizabayo, G., Chukwu, U.J., Abayeh, O.J. 2019. Extraction of Quercetin-Rich Red Onion Skin with Acetone and Chemical Modification using Aromatic Diazonium Salts. Makara J Sci. 23(2): 79–86, https://doi.org/10.7454/mss.v23i2.11045.

[57] Latiff, N., Ong, P.Y., Abdullah, L.C., Rashid, S.N.A.A., Fauzi, N.A.M., Amin, N.A.M. 2021. Ultrasonic-Assisted Extraction (UAE) for Enhanced Recovery of Bioactive Phenolic Compounds From *Cosmos caudatus* Leaves. Antioxid. 2020: 9, https://doi.org/10.21203/rs.3.rs-143469/v1.

[58] Torrecillas, C.M., Halbert, G.W., Lamprou, D.A., 2017. A Novel Methodology to Study Polymodal Particle Size Distributions Produced During Continuous Wet Granulation. Int. J. Pharm. 519: 230–239, https://doi.org/10.1016/j.ijpharm.2017.01.023.

[59] Zhu, J., Li, X., Liu, L., Li., Y., Qi, B., Jiang, L. 2021. Preparation of Spray-dried Soybean Oil Body Microcapsules using Maltodextrin: Effects of Dextrose Equivalence. LWT Food Sci. Technol. 15: 1–10, https://doi.org/10.1016/j.lwt.2021.112874.

[60] Wardhani, D.H., Wardana, I.N., Ulya, H.N., Cahyono, H., Kumoro, A.C., Aryanti, N. 2021. The Effect of Spray-drying Inlet Conditions in Iron Encapsulation using Hydrolysed Glucomannan as a Matrix. Food Bioprod. Process. 123: 72–79, https://doi.org/10.1016/j.fbp.2020.05.013.